



HHS Public Access

Author manuscript

Nat Struct Mol Biol. Author manuscript; available in PMC 2011 March 01.

Published in final edited form as:

Nat Struct Mol Biol. 2010 September ; 17(9): 1051–1057. doi:10.1038/nsmb.1868.

An Overlapping Kinase and Phosphatase Docking Site Regulates Activity of the Retinoblastoma Protein

Alexander Hirschi¹, Matthew Cecchini², Rachel C. Steinhardt³, Frederick A. Dick², and Seth M. Rubin^{3,*}

¹Department of Molecular, Cell, and Developmental Biology, University of California, Santa Cruz, CA 95064, USA

²London Regional Cancer Program, Children's Health Research Institute, and Department of Biochemistry, University of Western Ontario, London, Ontario N6A 4L6, Canada

³Department of Chemistry and Biochemistry, University of California, Santa Cruz, CA 95064, USA

Abstract

The phosphorylation state and corresponding activity of the retinoblastoma tumor suppressor protein (Rb) are modulated by a balance of kinase and phosphatase activities. Here we characterize the association of Rb with the catalytic subunit of protein phosphatase 1 (PP1c). A crystal structure identifies an enzyme-docking site in the Rb C-terminal domain that is required for efficient PP1c activity towards Rb. The phosphatase-docking site overlaps with the known docking site for Cyclin dependent kinase, and PP1 competition with Cdk-Cyclins for Rb binding is sufficient to retain Rb activity and block cell cycle advancement. These results provide the first detailed molecular insights into Rb activation and establish a novel mechanism for Rb regulation in which kinase and phosphatase compete for substrate docking.

The retinoblastoma tumor suppressor protein (Rb) regulates the cell cycle through its capacity to associate with and influence the function of a number of cellular proteins. In the best-characterized example, Rb binds and inhibits E2F transcription factors to coordinate the initiation of S phase with mitogenic signaling^{1,2}. Rb activity, namely its competency to bind E2F, is regulated by phosphorylation in a cell-cycle dependent manner. In G0 and early G1, Rb is active and modified at relatively few phosphorylation sites. In this hypophosphorylated state, Rb sequesters E2F and recruits transcriptional co-repressors and chromatin modifying enzymes to E2F responsive promoters to block transcription^{1,3–6}. Hyperphosphorylation of Rb by Cyclin-dependent kinases (Cdks) from late G1 until mitosis inactivates Rb by dissociating these factors and results in the expression of genes required

Users may view, print, copy, download and text and data- mine the content in such documents, for the purposes of academic research, subject always to the full Conditions of use: http://www.nature.com/authors/editorial_policies/license.html#terms

*Correspondence: srubin@ucsc.edu.

Author Contributions A.H., M.C., F.A.D., and S.M.R. all designed aspects of the study. A.H., M.C., R.C.S, and S.M.R. performed experiments. All authors analyzed data. F.A.D. and S.M.R. wrote the manuscript.

Accession Codes Protein Data Bank: Coordinates and structure factors for the Rb^{870–882}-PP1c complex have been deposited under code 3N5U.

for DNA synthesis and cell cycle progression^{1,7,8}. The enzyme protein phosphatase 1 (PP1), which is required for mitotic exit and is responsible for reversing the phosphorylation of many Cdk substrates, dephosphorylates Rb beginning in anaphase^{9–11}. PP1-dependent Rb dephosphorylation has also been observed during S and G2 in response to hypoxia and DNA damage, suggesting it is also responsible for Rb activation under these conditions^{12,13}. The importance of phosphorylation for regulating Rb activity as a tumor suppressor is underscored by the fact that genes encoding Cyclin D and p16 are frequently mutated in cancers leading to constitutive Rb hyperphosphorylation^{14,15}.

Mechanisms for regulating Rb phosphorylation have focused on the modulation of Cdk activity^{1,2,16}. While levels of Rb phosphorylation in the cell cycle generally coincide with levels of Cdk activity, there are circumstances, such as during mitotic exit and after DNA damage, in which Rb must be actively dephosphorylated and maintained in a hypophosphorylated state. Several cancer lines in fact have been shown to be defective in activating Rb by dephosphorylation¹⁷. Therefore, an important mechanistic question remains regarding how phosphatase activity opposes kinase activity to control Rb phosphorylation. A stable PP1-Rb complex has been observed that is coincident with the timing of dephosphorylation in mitosis¹⁸. Nevertheless, compared to Cdks, much less is known regarding how PP1 recognizes Rb and how Rb dephosphorylation may be regulated.

In cells, PP1 activity typically arises from a complex containing the catalytic subunit (PP1c) and a variable regulatory subunit; the latter confers substrate specificity and enhances activity¹⁹. There are three mammalian isoforms of PP1c; the isoforms all contain the highly conserved catalytic domain and only differ in their unstructured N- and C-termini^{19,20}. Nearly all regulatory subunits and many inhibitors contain a consensus 'RVxF' sequence, which binds PP1c at a site distinct from the catalytic site^{19–21}. Endogenous Rb-PP1 complexes copurify with other proteins, and an interaction between Rb and the myosin phosphatase targeting subunit has been reported^{22,23}; these observations suggest the existence of a regulatory subunit for Rb dephosphorylation. In contrast, there have been several reports of a direct, functional complex between Rb and all three PP1c isoforms without the requirement of a targeting subunit^{24,25}. Thus, the mechanism of Rb-specific PP1 activity remains unclear.

Rb contains two structured domains known as the N-terminal and pocket domains and a C-terminal domain (RbC) of approximately ~150 amino acids (Fig. 1a). RbC is necessary and sufficient for observation of an Rb-PP1c complex in cell extracts for all three PP1c isoforms^{24,25}. RbC is intrinsically disordered but adopts structure upon binding E2F-DP heterodimers (Supplementary Fig. 1)²⁶. Other proteins that have been shown to associate with RbC include Cyclins, Skp2, c-Abl, and MDM2^{27–30}. In the case of Cyclin A, a crystal structure reveals that a short RbC^{868–878} peptide docks to the structured Cyclin A domain in an extended conformation³¹. This sequence contains the canonical 'RxL' sequence motif that targets Cdk-Cyclins to Rb and other substrates for efficient phosphorylation^{27,32}. At present, little is known about whether these RbC binding partners are capable of interacting with Rb simultaneously or competitively, leaving their regulatory impact on Rb uncharacterized.

We examine here the RbC-PP1c association in molecular detail to understand the mechanism of Rb activation by dephosphorylation. We find that human PP1c uses its regulatory subunit-binding cleft to dock with an RVxF-like motif in RbC. The PP1c binding sequence overlaps with the previously identified RxL Cyclin binding site, and the association of Rb with PP1c and Cdk-Cyclin is exclusive. These results reveal an efficient regulatory mechanism, generally applicable in cell signaling, in which phosphatase and kinase activities not only affect phosphorylation state through catalysis, but also through restricting access to their target substrate.

Results

RbC^{870–882} is necessary and sufficient for PP1c association

To determine the precise sequence requirements for RbC-PP1c binding, we applied isothermal titration calorimetry to quantitate binding affinity. Recombinant, purified Rb proteins were titrated into recombinant PP1c (α -isoform), and dissociation constants were calculated from the resulting isotherms (Fig. 1). We first determined that Rb^{55–928}, which contains all of the conserved Rb domains and phosphoacceptor sites, binds PP1c with $K_d = 3.9 \pm 0.2 \mu\text{M}$ (Figs. 1b and 1c). This value is typical for enzyme-substrate binding interactions and is similar to that previously observed between an RbC peptide and Cyclin A³¹.

We next made a series of truncation mutants and tested the affinity of these mutants for PP1c by calorimetry (Fig. 1c and Supplementary Fig. 2). Rb^{771–928} and Rb^{866–928} bind to PP1c with similar affinity as full-length Rb, which is consistent with previous reports that RbC is sufficient for the association and phosphorylation is not required^{24,25,33}. Titration of Rb^{889–928} into PP1c results in no detectable heat signal, indicating that the conserved amino acid sequence between 866 and 889 is required for binding. Using a synthetic peptide, we found that Rb^{870–882} binds PP1c with comparable affinity ($K_d = 1.2 \pm 0.4 \mu\text{M}$) to full length Rb, confirming that Rb^{870–882} is necessary and sufficient for PP1c association and likely contains all of the significant interacting residues. This conserved sequence contains the Cyclin A docking site and a KLRF sequence that resembles the consensus RVxF motif found in PP1 regulatory subunits (Supplementary Fig. 1).

Crystal structure of Rb^{870–882}-PP1c

We next crystallized and solved the structure of a complex of the α -isoform of PP1c with an Rb^{870–882} peptide (Supplementary Information and Supplementary Fig. 3). The structure of PP1c in the complex is essentially identical to that observed in both the PP1c-microcystin and PP1c-tungstate complexes^{33,34}. The Rb peptide binds PP1c in an extended conformation at the hydrophobic interface of the core β -sandwich subdomain opposite the catalytic site (Fig. 2a). Rb binding is mediated both by mainchain hydrogen bonding and hydrophobic sidechain interactions (Figs. 2b and 2c). Arg876–Asp878 of Rb form a short β -strand that adds to sheet 1 of the PP1c β -sandwich subdomain. The Rb β -strand makes hydrogen-bonding interactions with the edge strand of the sheet that are typical of parallel strand-strand interactions.

The other significant interactions between the Rb peptide and PP1c are made by the highly conserved hydrophobic sidechains of Leu875 and Phe877 (Fig. 2c and Supplementary Fig. 1). Each inserts into a pocket within the hydrophobic core of the β -sandwich subdomain of PP1c. The PP1c β -sandwich structure and the specific sidechains that contact RbC are conserved in all three mammalian isoforms of the enzyme (Supplementary Fig. 4). Thus, our structural data are consistent with and explain the previous observation that all of the PP1c isoforms bind Rb²⁵. Furthermore, the observation that RbC contacts PP1c at a site that is distinct from the phosphatase active site explains the observation that catalytic activity of PP1c is not required for Rb-PP1 association³⁵.

The location of the Rb peptide binding site in PP1c and the molecular interactions stabilizing the complex are nearly identical to those observed between PP1c and the RVxF motif of two PP1 targeting subunits^{20,21}. In the structure of the myosin phosphatase subunit 1 (MYPT1) bound to PP1c (isoform δ) (Supplementary Fig. 5), Lys37-Asp39 of MYPT1 add to the PP1c sandwich domain as a parallel β -strand, and Val36 and Phe38 of MYPT1 insert into the same hydrophobic pockets of PP1c as observed here for Leu875 and Phe877 of Rb²⁰. Interestingly, the occurrence of leucine in RVxF motifs is extremely rare, and mutation of the canonical valine to leucine sometimes abolishes docking-motif binding³⁶. However, the similarity of contacts by RbC and MYPT1 with PP1 demonstrates that the KLRF sequence at amino acids 874–877 of Rb functions as an RVxF motif.

It is noteworthy that Leu875 and Phe877 in RbC also bind to hydrophobic pockets in CycA (Supplementary Figs. 1 and 5)³¹. Leu875 is the leucine in the Rb 'RxL' motif that is required for its phosphorylation^{27,31,32}. Phe877 is buried along with Leu875 in the RbC-Cdk2-CycA structure, and both appear critical for stabilizing the observed docking interaction between kinase and substrate³¹. We found that mutation of these hydrophobic residues results in a loss of RbC affinity for PP1c and Cdk2-CycA (Supplementary Information and Supplementary Fig. 2). These experiments verify that Leu875 and Phe877 are part of an enzyme-docking site in RbC required for association with both enzymes.

The Rb paralogs p107 and p130 also contain 'RxL' sequences that are critical for binding to Cdk2-CycA^{31,32}. However, unlike Rb, the phenylalanine in both the p107 and p130 docking motifs directly follows the leucine (RRLF). We found that the CycA binding motifs in both pocket proteins (p107^{655–667} and p130^{677–689}) do not also bind PP1c (Supplementary Fig. 2). This result is consistent with the crystal structure, which reveals that Leu forms critical contacts with PP1c in the –2 position (relative to the Phe).

PP1c docking is required for efficient RbC dephosphorylation

To examine the effects of the Rb-PP1c association on Rb-directed PP1 phosphatase activity, we developed an assay to measure Rb dephosphorylation rates. Two RbC constructs, both containing seven Cdk consensus sites (Fig. 3a), were quantitatively phosphorylated with ³²P. After mixing substrate with phosphatase, signal intensity remains at longer time points in phosRb^{771–874} compared to phosRb^{771–928} (Fig. 3b), indicating that deletion of the PP1c docking site in RbC results in loss of dephosphorylation efficiency. Quantification of the signal indicates that the first-order rate constant for dephosphorylation of phosRb^{771–874} ($k_{\text{dephos}} = 0.027 \pm 0.002 \text{ min}^{-1}$) is approximately eight times smaller than for phosRb^{771–928}

($k_{\text{dephos}} = 0.20 \pm 0.01 \text{ min}^{-1}$) (Fig. 3c). We also found that a short peptide containing the KLRF sequence inhibits phosRb⁷⁷¹⁻⁹²⁸ dephosphorylation when added to the assay, further confirming that the docking site permits more efficient substrate processing (Supplementary Fig. 6). Analogous phosphatase assays with mutant phosRbC fragments that contain only one pair of phosphorylated sites demonstrate that dephosphorylation occurs at all of the sites with kinetics that are sensitive to the presence of the PP1c docking site (Supplementary Fig. 7).

Phosphatase assays were performed at different substrate concentrations to determine apparent steady-state kinetic parameters for dephosphorylation of the multiple RbC sites (Fig. 3d). The apparent k_{cat} for dephosphorylation of phosRb⁷⁷¹⁻⁸⁷⁴ ($k_{\text{cat}} = 140 \pm 20 \text{ min}^{-1}$) and of phosRb⁷⁷¹⁻⁹²⁸ ($k_{\text{cat}} = 160 \pm 20 \text{ min}^{-1}$) are similar. However, the apparent K_{M} for phosRb⁷⁷¹⁻⁸⁷⁴ ($K_{\text{M}} = 30 \pm 10 \mu\text{M}$) is significantly greater than the apparent K_{M} of phosRb⁷⁷¹⁻⁹²⁸ ($K_{\text{M}} = 6 \pm 3 \mu\text{M}$). These results are consistent with the RbC KLRF docking sequence enhancing dephosphorylation by enabling PP1c to capture substrate and form an enzyme-substrate complex.

We next examined how mutations in the overlapping PP1c and Cdk-Cyclin docking site affect enzyme activity towards Rb. In the phosphatase assay, dephosphorylation of RbC⁷⁷¹⁻⁹²⁸ that contains an F877A mutation ($k_{\text{dephos}} = 0.071 \pm 0.004 \text{ min}^{-1}$) is significantly slower than wild type ($k_{\text{dephos}} = 0.29 \pm 0.03 \text{ min}^{-1}$) (Fig. 3e). Switching the position of the phenylalanine and arginine (R876F-F877R) in RbC⁷⁷¹⁻⁹²⁸, which creates a docking sequence that more resembles P107 and P130, also results in a smaller first-order rate constant in the assay ($k_{\text{dephos}} = 0.067 \pm 0.006 \text{ min}^{-1}$).

To test these mutants in a kinase assay, we prepared complexes of RbC and E2F1-DP1 to mimic the physiological, active Rb substrate. In binding assays, the presence of E2F1-DP1 does not affect appreciably the affinity of either PP1c or Cdk2-CycA for RbC (Supplementary Fig. 2), indicating that the E2F-DP binding site in RbC does not overlap with the common enzyme-docking site. The first-order rate constant characterizing phosphorylation of wild type RbC ($k_{\text{phos}} = 0.023 \pm 0.001 \text{ min}^{-1}$) is significantly greater than for the F877A mutant ($k_{\text{phos}} = 0.011 \pm 0.001 \text{ min}^{-1}$) (Fig. 3f). This measured kinetic difference is consistent with the KxLxF motif at 873-877 in Rb being required for phosphorylation by Cdk2-CycA²⁷. The R876F-F877R mutant ($k_{\text{phos}} = 0.024 \pm 0.001 \text{ min}^{-1}$) has a first-order rate constant similar to wild type. This observation follows previous findings that Cdk2-CycA is capable of docking to both K/RxLxF (Rb-like) or K/RxLF (P107-like) sequences³¹. Our kinetic studies of docking site mutants demonstrate that both PP1c and Cdk-Cyclin utilize an overlapping docking site in Rb and indicate that the R876F-F877R mutant is defective as a PP1 substrate but not as a Cdk substrate.

PP1 Inhibits Cdk2-CycA Activity Towards Rb

Considering that both kinase and phosphatase cannot bind the required docking site together, we hypothesized that each enzyme would act as an inhibitor of the other by occluding the site. We first tested whether inactive PP1c could inhibit the phosphorylation of RbC by Cdk2-CycA in the kinase assay (Fig. 4). In the absence of PP1c, the first-order rate constant for RbC⁷⁷¹⁻⁹²⁸ phosphorylation ($k_{\text{phos}} = 0.0185 \pm 0.0001 \text{ min}^{-1}$) was eleven times greater

than for RbC⁷⁷¹⁻⁸⁷⁴ phosphorylation ($k_{\text{phos}} = 0.0017 \pm 0.0001 \text{ min}^{-1}$). Kinase reactions were then carried out in the presence of saturating quantities of PP1c that was irreversibly inhibited at its catalytic site with microcystin (Fig. 4). The presence of PP1c-microcystin significantly reduces the rate constant for RbC⁷⁷¹⁻⁹²⁸ phosphorylation ($k_{\text{phos}} = 0.0051 \pm 0.0001 \text{ min}^{-1}$) such that it is more similar to the rate constant for RbC⁷⁷¹⁻⁸⁷⁴ phosphorylation. On the other hand, PP1c-microcystin has little effect on RbC⁷⁷¹⁻⁸⁷⁴ phosphorylation ($k_{\text{phos}} = 0.0013 \pm 0.0001 \text{ min}^{-1}$). Thus, our data indicate that PP1c directly inhibits RbC phosphorylation by Cdk2-CycA and that inhibition is independent of phosphatase activity and dependent on the presence of the KLRF docking site. We have also found using the phosphatase assay that Cdk2-CycA inhibits RbC directed PP1c phosphatase activity (Supplementary Fig. 8).

Inhibition of Cdk access to Rb blocks cell cycle progression

Having established that Cdk and PP1c compete for Rb access, we investigated the functional importance of this competition in the context of cell cycle regulation. The human osteosarcoma cell line Saos-2 is deficient for Rb, and Rb re-expression leads to a strong G1 arrest³⁷. Coexpression of Cdk2-CycA abrogates this arrest through phosphorylation and inactivation of Rb^{38,39}. We used this model system to observe the effect of PP1 on Cdk regulation of Rb (Fig. 5a). We found that the Rb induced arrest was overcome by Cdk2-CycA expression, and it could be largely recovered by expressing PP1c. Remarkably, co-expression of a catalytically inactive mutant of PP1c (PP1c-H248K) also resulted in a restoration of G1 arrest. Importantly, omission of Rb from these assays abrogates the PP1c dependent cell cycle block, confirming that Rb is the relevant target of enzyme competition. In Fig. 5b, the expression levels of PP1c were titrated and reveal that catalytically inactive enzyme is as potent as wild type in blocking cell cycle advancement under conditions in which Rb expression has been reduced. Based on these cell cycle control data, we conclude that the competition for substrate access between Cdk2-CycA and PP1c on Rb offers an efficient means to control cell proliferation beyond the catalytic regulation of phosphorylation.

We next confirmed that PP1c inhibits phosphorylation of Rb in cells, as in our kinetic analyses, in a manner that is independent of catalytic activity. We used C33A cells to test whether exogenously introduced PP1c could compete with Cdks and block Rb phosphorylation regardless of cell cycle position effects on enzyme activity (Fig. 5c). Ectopically expressed Rb becomes phosphorylated in C33A cells. Expression of a dominant negative Cdk2 controls for inhibition of Rb phosphorylation in our analysis, and co-expression of Rb with Cdk2-CycA demonstrates the maximum extent of Rb hyperphosphorylation. As predicted, expression of PP1c or catalytically dead PP1c-H248K inhibited Rb phosphorylation levels in a dose dependent manner.

Our kinetic data indicate that the Rb^{R876F-F877R} mutant is a poor PP1 substrate but a good Cdk substrate. We used this mutation to study the importance of the docking site for dephosphorylation and Rb activation in cell based assays. First, we transfected wild type Rb and Rb^{R876F-F877R} into C33A cells with and without also transfecting PP1c (Fig. 5d). Co-expression of PP1c reduces the observed phosphorylation of wild-type Rb (migrates as a

faster, single band), while the mutant Rb^{R876F-F877R} is unaffected by phosphatase expression. This observation suggests that the docking interaction observed in our crystal structure is required in cells for efficient Rb dephosphorylation by PP1.

We also tested the Rb^{R876F-F877R} mutant in the Saos-2 cell cycle arrest assay. Expression of Rb^{R876F-F877R} in Saos-2 cells gives a less robust arrest in G1 compared to wild-type, consistent with the idea that Rb activation requires docking-dependent PP1c dephosphorylation that is defective in this mutant (Fig. 5e). Cdk2-CycA expression still inactivates Rb^{R876F-F877R} as expected, because the kinase-docking site remains intact. We also find that under conditions in which Rb and kinase are expressed, co-expression of PP1c is sufficient to restore the activity of WT-Rb but is unable to reactivate phosphorylated Rb^{R876F-F877R} (Fig. 5f). Taken together these data highlight a critical role for the KLRF docking site in the regulation of Rb activity.

Stable Rb-PP1 complexes are coincident with Rb activation

The competition for access to Rb between PP1c and Cdk-Cyclin suggests that Rb and PP1c are in a complex at times when Rb is activated by dephosphorylation. To investigate the relevance of this mechanism of cell cycle regulation under endogenous conditions, we compared the abundance of Rb and PP1 complexes in CV-1 cells during mitotic exit and transfected Saos-2 cells that arrest in a PP1 dependent manner in early G1 (Fig. 6). We utilized CV-1 cells because synchronization experiments have shown that PP1 and Rb associate selectively in late mitosis coincident with Rb dephosphorylation and activation in these cells¹⁸. We first compared the relative level of the endogenous proteins in CV-1 cells with the level of transfected proteins in Saos-2 cells by applying recombinant standards (Fig. 6a). We found that the molar quantities of Rb in extracts from CV-1 and Saos-2 transfected cells were equivalent. Considering that the majority of Saos-2 cells are transfected in our experiments, the Rb expression level in the Saos-2 cells is no more than 2 times higher. The levels of PP1 in mitotic CV-1 cells were a little less than half as much as Rb, whereas the total levels of endogenous and exogenously introduced PP1 in arrested Saos-2 cells was approximately equivalent to Rb. These observations indicate that our transfection based assay system closely mimics the levels of endogenous proteins under conditions where Rb is activated.

We next immunoprecipitated Rb complexes from CV-1 and transfected Saos-2 cells and immunoblotted for bound PP1 (Fig. 6b). The amount of PP1 co-precipitated from arrested Saos-2 cells is approximately 30% of the total amount of immunoprecipitated Rb, indicating that a third of Rb molecules are bound to PP1 when cells are arrested in a PP1 dependent manner. The amount of PP1 co-precipitated with Rb in CV-1 cells is approximately 2%; however, given that the population of CV-1 cells is actively progressing through mitosis and the limitations of synchronization by shake-off, this measurement likely underestimates the quantity of Rb-PP1 complex that exists in a cell at the instant of Rb activation. Taken together these experiments suggest that PP1 can form stable, abundant complexes with Rb at endogenous expression levels. These complexes attenuate the activity of Cdks by blocking their access to Rb and regulate progression through the cell cycle.

Discussion

While much attention has been paid to the inactivation of Rb by Cdk phosphorylation from G1 through mitosis, less is known regarding how Rb is activated by PP1 dephosphorylation during mitotic exit and following cellular stress. We have identified a short sequence in RbC that binds to PP1c directly and is required for efficient Rb-directed PP1 phosphatase activity. Our structural data demonstrate that the molecular interactions stabilizing RbC-PP1c are nearly identical to those observed between PP1c and its regulatory subunits. Whereas PP1c typically uses its hydrophobic binding cleft to recruit an additional subunit responsible for substrate binding, here PP1c uses the cleft to recruit Rb substrate directly^{20,21}. Although uncommon, a direct interaction between PP1c and the PP1 substrate Cdc25 has also been observed in *Xenopus* embryonic extracts⁴⁰. Recent data indicate that PP1c dissociates from inhibitors following Cdk inactivation during mitosis⁹. The timing of this population of free PP1c is concurrent with the requirement to dephosphorylate Rb through a direct interaction, and it would be interesting to explore whether other PP1 substrates are dephosphorylated at mitotic exit without a targeting subunit.

The fact that the direct enzyme-substrate association is mediated through the 'RVxF'-binding cleft may explain why an Rb targeting regulatory subunit has not been identified and is not necessary for Rb dephosphorylation²⁵. While the existence of such a subunit cannot be ruled out, our data indicate that both Rb and a hypothetical Rb-targeting subunit could not both occupy the 'RVxF'-binding cleft and that a different mode of Rb-PP1 holoenzyme assembly would be required. However, considering that multiple phosphates in varying sequence contexts must be hydrolyzed in Rb, it seems reasonable that the Rb phosphatase would not employ a targeting subunit to impart a high degree of specificity. RbC closely mimics regulatory subunits in PP1 binding, and it is also tempting to speculate that Rb itself is a PP1 regulatory subunit, either sequestering nuclear PP1c from other activating subunits or regulating PP1c access to other substrates. Interestingly, it has been reported that RbC can act as a noncompetitive inhibitor of PP1c activity towards a generic substrate³⁵.

Our data together with previous results indicate that PP1c and Cdk2-CycA bind to an overlapping docking site in RbC that is required in each case for efficient enzymatic activity^{27,31}. To our knowledge, this observation is the first example of a PP1c binding sequence (RVxF or other) having an additional functional role that competes with PP1 activity. As a result of their exclusive associations with substrate, we have demonstrated that Cdk2-CycA and PP1c can each directly inhibit the activity of the other enzyme towards Rb. This result reveals a novel mechanism for the regulation of Rb phosphorylation state in which kinase and phosphatase compete for access to substrate. Given the conservation of the RxL binding cleft in Cyclin paralogs, it is assumed that the observed competition would exist between PP1 and all Cdk-Cyclins that phosphorylate Rb. In contrast, the other Rb family proteins p107 and p130 do not bind PP1c; this competitive mechanism is unique to Rb.

Competition between kinase and phosphatase for controlling the phosphorylation state of a common substrate has been established as an important mechanism in cell signaling, and a

theoretical framework has been crafted for how such competition can generate critical signaling properties such as sensitivity, switch-like responses, and multiple steady state outputs^{41–44}. However, few experimental observations of these properties have been reported. Our finding of a Cdk-Cyclin competition with PP1c for Rb as a substrate not only provides a rare example of direct kinase/phosphatase competition, but also demonstrates that competition can be for substrate docking as well as catalysis. Interestingly, the presence of common kinase/phosphatase docking sites in MAP kinases have been observed⁴⁵, suggesting that competition for substrate binding may play a more general role in signal transduction.

In the context of Rb phosphorylation in cell cycle control, signaling sensitivity and specificity are critical. From mitosis through G1, the capacity of PP1c to inhibit Cdk-Cyclin could facilitate efficient Rb dephosphorylation in response to small changes in PP1c concentration and prevent Rb from being promiscuously rephosphorylated by residual Cdk activity. The same holds true in response to cellular stress and cell cycle exit, and in fact, it has been shown that Rb is dephosphorylated in response to DNA damage despite the presence of active Cdks¹³. These regulatory concepts that would serve to activate Rb are supported by our cell cycle arrest assays. Therefore, our findings establish a biochemical mechanism through which Rb phosphorylation and function can be tightly controlled in the cell by directly competing kinase and phosphatase activities. Further study is necessary to determine what mechanisms influence the outcome of the competition and how access of each enzyme to the docking site is controlled. Considering the observation that the association between Rb and PP1c is direct, the nuclear concentration of PP1c, free of inhibitors and other targeting subunits, is an intriguing possible factor.

Methods

Protein Expression and Purification

Recombinant PP1c (α isoform) was expressed in *E. coli* using a *tac* promoter; 2 mM $MnCl_2$ was added to the media upon induction. Purification was best achieved utilizing a salt-dependent PP1c-inhibitor-2 association⁴⁶. Full-length, human inhibitor-2 was expressed with an N-terminal 6xHis tag in *E. coli*. Following cell lysis with 6M urea, inhibitor-2 was bound to nickel sepharose beads and exchanged to a buffer containing 20 mM Tris, 50 mM NaCl, 15 mM imidazole, 0.4 mM $MnCl_2$, 0.2 mM TCEP, and 0.1 mM PMSF (pH 8.0). Cells expressing PP1c were lysed in this same buffer, the cleared lysate was passed over the immobilized inhibitor-2, and PP1c was eluted with lysis buffer containing 1 M NaCl. For crystallography, PP1c was further purified with a Superdex75 column (GE Healthcare) equilibrated in 20 mM Tris, 500 mM NaCl, 2 mM DTT, 0.4 mM $MnCl_2$ (pH 8.0). RbC, Rb^{55–928}, E2F1-DP1 (RbC binding domains), and Cdk2-CycA protein constructs were expressed and purified as described previously^{26,47,48}. The Rb constructs in both the calorimetry and kinetic experiments had N-terminal 6xHis tags left intact. Cdk activating kinase from *Saccharomyces cerevisiae* (Cak) was expressed as a GST fusion protein in *E. coli* and purified with glutathione sepharose affinity chromatography.

Isothermal Titration Calorimetry

Isothermal titration calorimetry experiments were performed with a VP-ITC instrument (MicroCal). Typically, 0.5–1 mM of each RbC construct or synthetic RbC peptide was titrated into a 25–50 μM solution of PP1c. Experiments were carried out at 25°C in a buffer containing 25 mM Tris, 100 mM NaCl, and 1 mM DTT (pH 8.0). Each reported binding constant is the average from 2–3 experiments, and the reported error is the standard deviation of the K_d from these measurements.

Crystallization and Structure Determination

Purified PP1c was concentrated to 10 mg mL⁻¹ after the Superdex75 column and synthetic RbC^{870–882} peptide (Biopeptide Co., Inc.) was added in a 3:1 molar ratio. Crystals were grown using the hanging-drop vapor diffusion method at room temperature. The crystallization buffer contained 100 mM Hepes, 200 mM MgCl₂, and 18% Peg 4K (pH 7.5) and was mixed in a 1:1 ratio with protein solution. Crystals grew with a needle morphology to dimensions of approximately 50 μm \times 50 μm \times 500 μm . Crystals were harvested by transferring to a solution containing 100 mM Hepes, 200 mM MgCl₂, 20% Peg 4K, and 20% glycerol (pH 7.5) and flash freezing in liquid nitrogen. A molecular replacement solution was obtained using the PP1c-microcystin crystal structure (PDB ID: 1fjm) as a search model³⁴. Further details regarding model building and refinement can be found in Supplementary Methods.

Phosphatase and Kinase Assays

Purified Cdk2-CycA was first activated by phosphorylation in a reaction containing 10% w/w GST-Cak, 10 mM MgCl₂, and 5 mM ATP. To prepare for the phosphatase assays, 1 mg of RbC was incubated with 0.25 mg of activated Cdk2-CycA for 1 hour at room temperature in a buffer containing 50 mM Hepes, 100 mM NaCl, 10 mM MgCl₂, 1 mM ATP, and 5 μCi of ³²P-ATP (pH 7.5). These reaction conditions give nearly quantitative phosphorylation of Cdk consensus sites in RbC⁴⁸. Reactions were quenched by addition of 8M urea, and phosRbC was isolated with a Ni²⁺-NTA spin column (Qiagen). Phosphatase reactions were carried out at room temperature in a buffer containing 50 mM Hepes, 100 mM NaCl, 2 mM MnCl₂ (pH 7.5). Reactions were initiated by addition of enzyme. Aliquots were removed at the indicated time point and quenched by mixing with SDS-PAGE loading buffer.

For the phosphatase steady-state analysis, dephosphorylation assays were carried out at varying substrate concentrations. The initial rate at each concentration was determined from a linear fit of band intensities of the first 3–4 time points, and the corresponding fitting errors were assigned as the error of each rate measurement. Initial rates were fit as a function of substrate concentration with a simple Michaelis-Menten model to calculate the effective K_M and k_{cat} .

For kinase assays, 75 nM activated (phosphorylated with CAK) Cdk2-CycA, 20 μM E2F1-DP1, and 2 μM RbC substrates were mixed in a reaction at room temperature containing the kinase buffer described above and 20 μCi of ³²P-ATP (pH 7.5). In kinase reactions with PP1c, PP1c was first inactivated by mixing in a 1:3 molar ratio with L,R-microcystin. An additional 25 μM microcystin was present in the competition reactions to ensure no residual

PP1c activity (the IC₅₀ for microcystin is ~1 nM). Phosphorimaging was done with a Typhoon Trio gel scanner (Amersham) and data analyzed with the ImageQuant software package (Molecular Dynamics). Kinetic data were fit with a first-order rate law using Kaleidagraph. The reported error of each kinetic parameter is the fitting error.

Cell cycle arrest experiments

Saos-2 cells were cultured according to standard methods. 1×10^6 proliferating cells were transfected with 0.75 μg of CMV-Rb (0.5 μg in Fig. 5b), 1 μg of CMV-CD20 (used to mark transfected cells in flow cytometry analysis) and 6 μg of CMV-bGal, using Fugene 6 (Roche). Where indicated, 1 μg of CMV-HA-cdk2, 1 μg of CMV-cyclin A, and 4 μg of CMV-myc-PP1c were added and the appropriate amount of CMV-bGal was omitted to maintain uniform DNA concentrations. Three days following transfection cells were analyzed by flow cytometry as described previously⁴⁹.

C33A cells were transfected with 10 μg of CMV-Rb, 2.5 μg of CMV-HA-cdk2, 2.5 μg of CMV cyclin A, and 2.5 to 10 μg of CMV-myc-PP1c; CMV- β Gal was included where necessary to obtain a final quantity of 25 μg . Transfections were performed by Ca₂PO₄ precipitation. Cells were harvested after 2 days and nuclear lysates prepared for SDS-PAGE and western blotting as described⁵⁰. Rb was detected with monoclonal antibody G3-245 (BD Pharmingen) and anti-phosphoserine 807/811 antibodies from Cell Signaling.

For immunoprecipitation experiments, extracts were prepared as described above from Saos-2 cells transfected with Fugene HD (Roche). CV-1 cells were isolated by mitotic shake-off from cultures that were first blocked in S-phase with 2.5 mg/mL aphidicolin for 24 hours then released for 16 hours to enrich for mitotic cells. Immunoprecipitations were carried out using monoclonal antibody Rb4.1 (Developmental Studies Hybridoma Bank at the University of Iowa) against Rb. Extracts and immunoprecipitated proteins were analyzed by SDS-PAGE alongside recombinant PP1c and GST-Rb³⁸⁰⁻⁹²⁸ controls. Rb and PP1 were detected on western blots by Rb4.1 and sc-7482 (Santa Cruz) respectively. Standard curves to determine protein quantities were generated by using Image J software (NIH) to quantitate band intensities.

Supplementary Material

Refer to Web version on PubMed Central for supplementary material.

Acknowledgements

The authors acknowledge the staff at Beamline 5.0.1 of the Advanced Light Source (Lawrence Berkeley National Laboratories) and are grateful to N. Dyson (MGH, Boston) for CMV-CycA and T. Pawson (MSHRI, Toronto) for the CMV-myc-PP1c plasmid. The Rb 4.1 hybridoma developed by J. Sage was obtained from the Developmental Studies Hybridoma Bank developed under the auspices of the NICHD and maintained by The University of Iowa, Department of Biology, Iowa City, IA 52242. This work is supported by grants from the Canadian Institutes of Health Research (MOP89765 to F.A.D.) and the National Institutes of Health (R01CA132685 to S.M.R.). A.H. is supported by an NIH training grant (T32GM008646). M.C. acknowledges the CIHR for an M.D./Ph.D. studentship award and the CaRTT training program. F.A.D. thanks the Canadian Cancer Society for a Research Scientist Award. S.M.R. is a Pew Scholar in the Biomedical Sciences.

References

1. Dyson N. The regulation of E2F by pRB-family proteins. *Genes Dev.* 1998; 12:2245–62. [PubMed: 9694791]
2. Weinberg RA. The retinoblastoma protein and cell cycle control. *Cell.* 1995; 81:323–30. [PubMed: 7736585]
3. Brehm A, et al. Retinoblastoma protein recruits histone deacetylase to repress transcription. *Nature.* 1998; 391:597–601. [PubMed: 9468139]
4. Kennedy BK, et al. Histone deacetylase-dependent transcriptional repression by pRB in yeast occurs independently of interaction through the LXCXE binding cleft. *Proc Natl Acad Sci USA.* 2001; 98:8720–5. [PubMed: 11447271]
5. Nielsen SJ, et al. Rb targets histone H3 methylation and HP1 to promoters. *Nature.* 2001; 412:561–5. [PubMed: 11484059]
6. Zhang HS, et al. Exit from G1 and S phase of the cell cycle is regulated by repressor complexes containing HDAC-Rb-hSWI/SNF and Rb-hSWI/SNF. *Cell.* 2000; 101:79–89. [PubMed: 10778858]
7. Adams PD. Regulation of the retinoblastoma tumor suppressor protein by cyclin/cdks. *Biochim Biophys Acta.* 2001; 1471:M123–33. [PubMed: 11250068]
8. Harbour JW, Luo RX, Dei Santi A, Postigo AA, Dean DC. Cdk phosphorylation triggers sequential intramolecular interactions that progressively block Rb functions as cells move through G1. *Cell.* 1999; 98:859–69. [PubMed: 10499802]
9. Wu JQ, et al. PP1-mediated dephosphorylation of phosphoproteins at mitotic exit is controlled by inhibitor-1 and PP1 phosphorylation. *Nat Cell Biol.* 2009; 11:644–51. [PubMed: 19396163]
10. Ludlow JW, Glendening CL, Livingston DM, DeCaprio JA. Specific enzymatic dephosphorylation of the retinoblastoma protein. *Mol Cell Biol.* 1993; 13:367–72. [PubMed: 8380224]
11. Ludlow JW, Shon J, Pipas JM, Livingston DM, DeCaprio JA. The retinoblastoma susceptibility gene product undergoes cell cycle-dependent dephosphorylation and binding to and release from SV40 large T. *Cell.* 1990; 60:387–96. [PubMed: 2154332]
12. Krucher NA, et al. Dephosphorylation of Rb (Thr-821) in response to cell stress. *Exp Cell Res.* 2006; 312:2757–63. [PubMed: 16764854]
13. Dou QP, An B, Will PL. Induction of a retinoblastoma phosphatase activity by anticancer drugs accompanies p53-independent G1 arrest and apoptosis. *Proc Natl Acad Sci U S A.* 1995; 92:9019–23. [PubMed: 7568064]
14. Classon M, Harlow E. The retinoblastoma tumour suppressor in development and cancer. *Nat Rev Cancer.* 2002; 2:910–7. [PubMed: 12459729]
15. Sherr CJ. Cancer cell cycles. *Science.* 1996; 274:1672–7. [PubMed: 8939849]
16. Morgan DO. Principles of CDK regulation. *Nature.* 1995; 374:131–4. [PubMed: 7877684]
17. Broceno C, Wilkie S, Mittnacht S. RB activation defect in tumor cell lines. *Proc Natl Acad Sci U S A.* 2002; 99:14200–5. [PubMed: 12379745]
18. Durfee T, et al. The retinoblastoma protein associates with the protein phosphatase type 1 catalytic subunit. *Genes Dev.* 1993; 7:555–69. [PubMed: 8384581]
19. Cohen PT. Protein phosphatase 1--targeted in many directions. *J Cell Sci.* 2002; 115:241–56. [PubMed: 11839776]
20. Terrak M, Kerff F, Langsetmo K, Tao T, Dominguez R. Structural basis of protein phosphatase 1 regulation. *Nature.* 2004; 429:780–4. [PubMed: 15164081]
21. Egloff MP, et al. Structural basis for the recognition of regulatory subunits by the catalytic subunit of protein phosphatase 1. *Embo J.* 1997; 16:1876–87. [PubMed: 9155014]
22. Kiss A, et al. Myosin phosphatase interacts with and dephosphorylates the retinoblastoma protein in THP-1 leukemic cells: its inhibition is involved in the attenuation of daunorubicin-induced cell death by calyculin-A. *Cell Signal.* 2008; 20:2059–70. [PubMed: 18755268]
23. Nelson DA, Krucher NA, Ludlow JW. High molecular weight protein phosphatase type 1 dephosphorylates the retinoblastoma protein. *J Biol Chem.* 1997; 272:4528–35. [PubMed: 9020179]

24. Tamrakar S, Ludlow JW. The carboxyl-terminal region of the retinoblastoma protein binds non-competitively to protein phosphatase type 1 α and inhibits catalytic activity. *J Biol Chem.* 2000; 275:27784–9. [PubMed: 10889204]
25. Vietri M, Bianchi M, Ludlow JW, Mittnacht S, Villa-Moruzzi E. Direct interaction between the catalytic subunit of Protein Phosphatase 1 and pRb. *Cancer Cell Int.* 2006; 6:3. [PubMed: 16466572]
26. Rubin SM, Gall AL, Zheng N, Pavletich NP. Structure of the Rb C-terminal domain bound to E2F1-DP1: a mechanism for phosphorylation-induced E2F release. *Cell.* 2005; 123:1093–106. [PubMed: 16360038]
27. Adams PD, et al. Retinoblastoma protein contains a C-terminal motif that targets it for phosphorylation by cyclin-cdk complexes. *Mol Cell Biol.* 1999; 19:1068–80. [PubMed: 9891042]
28. Ji P, et al. An Rb-Skp2-p27 pathway mediates acute cell cycle inhibition by Rb and is retained in a partial-penetrance Rb mutant. *Mol Cell.* 2004; 16:47–58. [PubMed: 15469821]
29. Welch PJ, Wang JY. A C-terminal protein-binding domain in the retinoblastoma protein regulates nuclear c-Abl tyrosine kinase in the cell cycle. *Cell.* 1993; 75:779–90. [PubMed: 8242749]
30. Xiao ZX, et al. Interaction between the retinoblastoma protein and the oncoprotein MDM2. *Nature.* 1995; 375:694–8. [PubMed: 7791904]
31. Lowe ED, et al. Specificity determinants of recruitment peptides bound to phospho-CDK2/cyclin A. *Biochemistry.* 2002; 41:15625–34. [PubMed: 12501191]
32. Schulman BA, Lindstrom DL, Harlow E. Substrate recruitment to cyclin-dependent kinase 2 by a multipurpose docking site on cyclin A. *Proc Natl Acad Sci U S A.* 1998; 95:10453–8. [PubMed: 9724724]
33. Egloff MP, Cohen PT, Reinemer P, Barford D. Crystal structure of the catalytic subunit of human protein phosphatase 1 and its complex with tungstate. *J Mol Biol.* 1995; 254:942–59. [PubMed: 7500362]
34. Goldberg J, et al. Three-dimensional structure of the catalytic subunit of protein serine/threonine phosphatase-1. *Nature.* 1995; 376:745–53. [PubMed: 7651533]
35. Tamrakar S, Mittnacht S, Ludlow JW. Binding of select forms of pRB to protein phosphatase type 1 independent of catalytic activity. *Oncogene.* 1999; 18:7803–9. [PubMed: 10618721]
36. Meiselbach H, Sticht H, Enz R. Structural analysis of the protein phosphatase 1 docking motif: molecular description of binding specificities identifies interacting proteins. *Chem Biol.* 2006; 13:49–59. [PubMed: 16426971]
37. Huang HJ, et al. Suppression of the neoplastic phenotype by replacement of the RB gene in human cancer cells. *Science.* 1988; 242:1563–6. [PubMed: 3201247]
38. Hinds PW, et al. Regulation of retinoblastoma protein functions by ectopic expression of human cyclins. *Cell.* 1992; 70:993–1006. [PubMed: 1388095]
39. Zhu L, et al. Inhibition of cell proliferation by p107, a relative of the retinoblastoma protein. *Genes Dev.* 1993; 7:1111–25. [PubMed: 8319904]
40. Margolis SS, et al. PP1 control of M phase entry exerted through 14-3-3-regulated Cdc25 dephosphorylation. *Embo J.* 2003; 22:5734–45. [PubMed: 14592972]
41. Ferrell JE Jr. Tripping the switch fantastic: how a protein kinase cascade can convert graded inputs into switch-like outputs. *Trends Biochem Sci.* 1996; 21:460–6. [PubMed: 9009826]
42. Goldbeter A, Koshland DE Jr. An amplified sensitivity arising from covalent modification in biological systems. *Proc Natl Acad Sci U S A.* 1981; 78:6840–4. [PubMed: 6947258]
43. Salazar C, Hofer T. Competition effects shape the response sensitivity and kinetics of phosphorylation cycles in cell signaling. *Ann N Y Acad Sci.* 2006; 1091:517–30. [PubMed: 17341641]
44. Thomson M, Gunawardena J. Unlimited multistability in multisite phosphorylation systems. *Nature.* 2009; 460:274–7. [PubMed: 19536158]
45. Tanoue T, Adachi M, Moriguchi T, Nishida E. A conserved docking motif in MAP kinases common to substrates, activators and regulators. *Nat Cell Biol.* 2000; 2:110–6. [PubMed: 10655591]

46. Zhang Z, Zhao S, Zirattu SD, Bai G, Lee EY. Expression of recombinant inhibitor-2 in *E. coli* and its utilization for the affinity chromatography of protein phosphatase-1. *Arch Biochem Biophys.* 1994; 308:37–41. [PubMed: 8311471]
47. Russo AA. Purification and reconstitution of cyclin-dependent kinase 2 in four states of activity. *Methods Enzymol.* 1997; 283:3–12. [PubMed: 9251007]
48. Burke JR, Deshong AJ, Pelton JG, Rubin SM. Phosphorylation-induced conformational changes in the retinoblastoma protein inhibit E2F transactivation domain binding. *J Biol Chem.* 2010; 285:16286–93. [PubMed: 20223825]
49. van den Heuvel S, Harlow E. Distinct roles for cyclin-dependent kinases in cell cycle control. *Science.* 1993; 262:2050–4. [PubMed: 8266103]
50. Seifried LA, et al. pRB-E2F1 complexes are resistant to adenovirus E1A-mediated disruption. *J Virol.* 2008; 82:4511–20. [PubMed: 18305049]

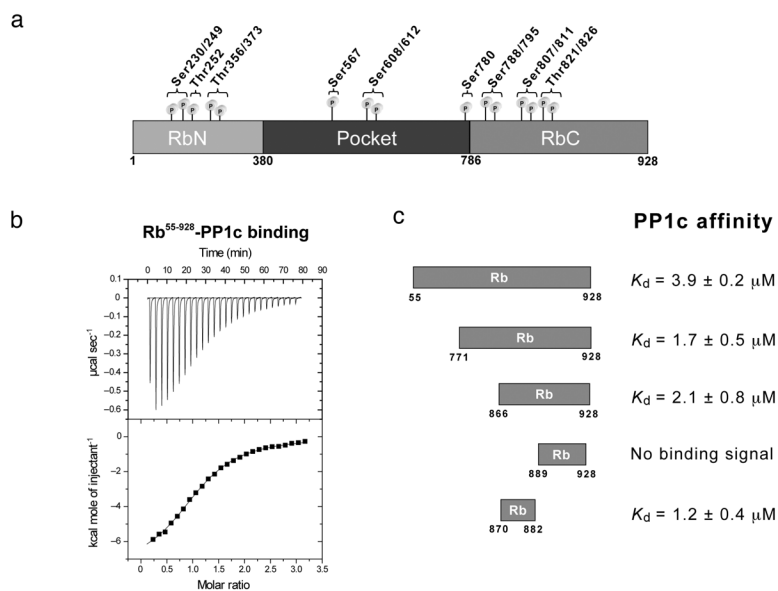


Figure 1. Rb⁸⁸⁰⁻⁸⁹² is necessary and sufficient for RbC-PP1c association. **(a)** Domain structure of Rb with the location of the conserved Cdk consensus phosphorylation sites. **(b)** Isothermal titration calorimetry (ITC) data for titration of Rb⁵⁵⁻⁹²⁸ into PP1c. **(c)** Results from ITC experiments as shown in (a) but with RbC truncation mutants. Sample ITC data from each experiment are shown in Supplementary Fig. 2.

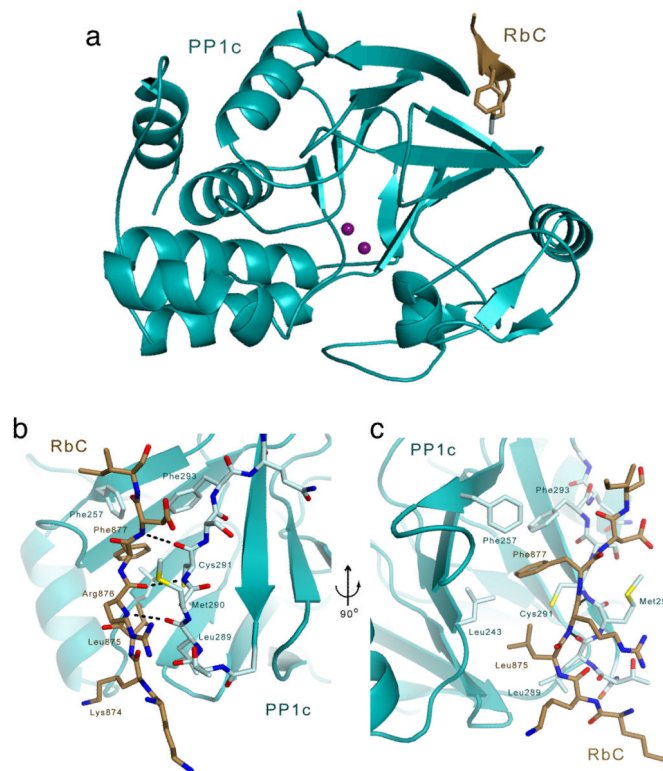


Figure 2.

Structure of the RbC⁸⁷⁰⁻⁸⁸²-PP1c complex. (a) RbC (brown) binds in an extended conformation and extends sheet 1 of the PP1c β -sandwich domain (cyan). The Mn²⁺ ions at the distant PP1c catalytic site are shown as purple spheres. (b) Close up of RbC⁸⁷⁰⁻⁸⁸²-PP1c interface. The mainchain hydrogen bonding interactions, between the RbC peptide (light brown) and PP1c (cyan) are shown. (c) Hydrophobic sidechain interactions between RbC⁸⁷⁰⁻⁸⁸² and PP1c.

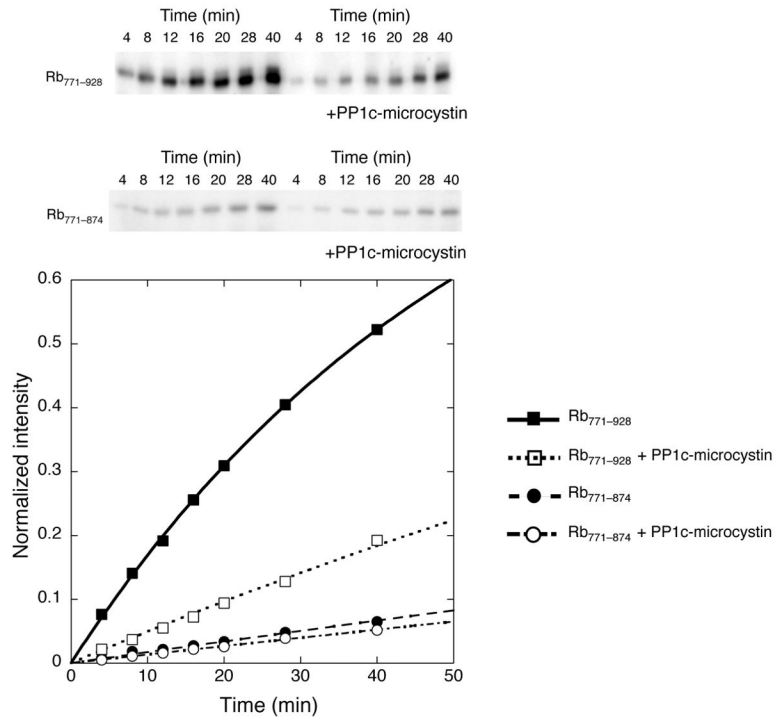
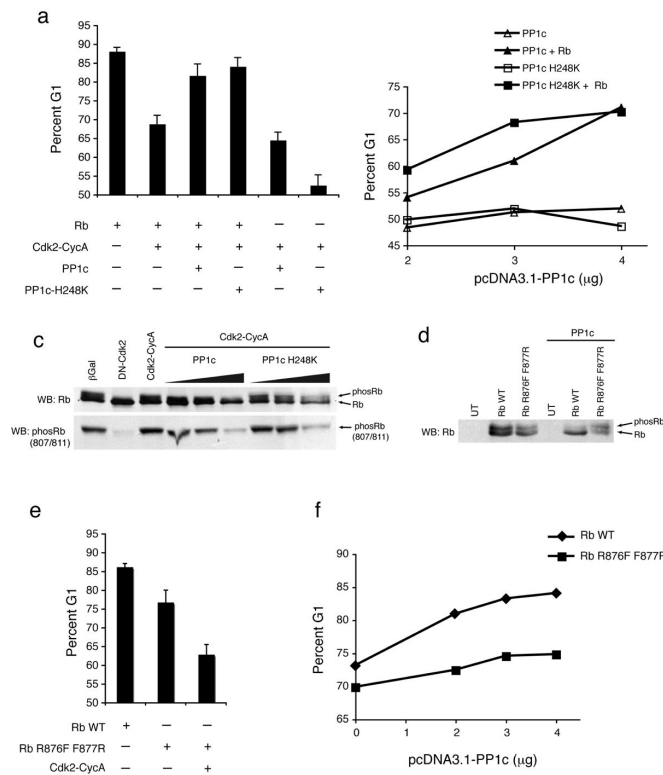
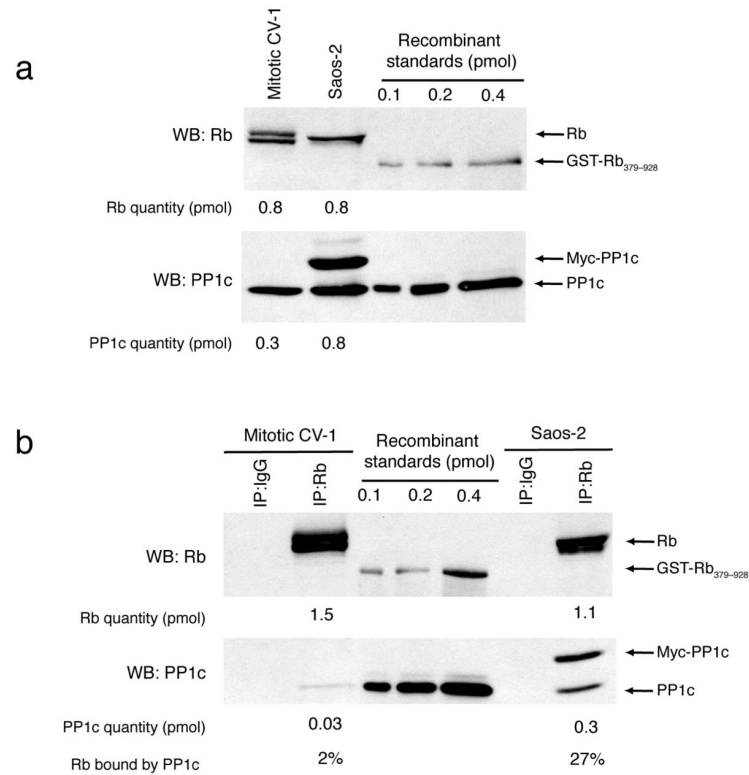


Figure 4. PP1c inhibits Cdk2-CycA activity towards RbC. Phosphorylation of 2 μM RbC⁷⁷¹⁻⁹²⁸ or RbC⁷⁷¹⁻⁸⁷⁴ with 75 nM Cdk2-CycA in the absence (v,λ) and presence (□,○) of a saturating concentration of PP1c-microcystin (15 μM).

**Figure 5.**

PP1c inhibits Cdk inactivation of Rb independent of phosphatase activity. **(a)** Saos-2 cells were transfected with expression plasmids corresponding to the indicated proteins. The H248K form of PP1 is a catalytically inactive mutant. The percentage of cells in G1 is indicated for each. Error bars represent one standard deviation from the mean from at least four experiments. **(b)** Saos-2 cells were again transfected with Cdk2-CycA, and Rb expression plasmids and cell cycle position was analyzed by flow cytometry. The levels of expression plasmid for PP1 and the H248K mutant were titrated to compare their relative effect on an Rb dependent arrest. **(c)** C33A cells were transfected with the expression plasmids corresponding to the indicated proteins. Rb and phosphoserine 807/811-Rb were detected by western blotting. The relative migration positions of hyper- and hypophosphorylated Rb are indicated as phosRb and Rb respectively. **(d)** C33A cells were transfected with the indicated proteins and Rb was detected as in (c). **(e)** Saos-2 cells were transfected with expression plasmids corresponding to the indicated proteins, and the analysis was conducted as in (a). **(f)** Saos-2 cells were transfected with Rb, or the indicated Rb mutant, and Cdk2-CycA expression plasmids as in (b). Increasing quantities of PP1c were co-transfected to assess the sensitivity of the Rb mutant to protection from phosphorylation and subsequent cell cycle advancement out of the G1 phase.

**Figure 6.**

Abundant Rb-PP1c complexes during PP1c dependent growth arrest. **(a)** Saos-2 cells were transfected as in Fig. 5a to generate a PP1c dependent arrest in early G1. CV-1 cells were released from a S-phase block and mitotic cells were isolated by a mitotic shake-off 16 hours later. Extracts were analyzed by SDS-PAGE and western blotting to quantitate Rb and PP1c levels. Quantities of Rb and PP1c were determined by band intensities relative to a standard curve generated using recombinant proteins. The quantities are listed below each respective gel lane. **(b)** Rb was immunoprecipitated from extracts prepared as in (a), and the quantities of Rb and associated PP1c were determined as above.

Table 1

X-ray data collection and structure model refinement statistics

	Rh⁸⁷⁰⁻⁸⁸²-PP1c
Data Collection	
Space group	P4 ₁ 2 ₁ 2
Cell dimensions	
<i>a</i> , <i>b</i> , <i>c</i> (Å)	92.95, 92.95, 192.38
α, β, γ (°)	90, 90, 90
Resolution (Å)	83.6–3.2
R _{pim} (%) ^a	5.6 (20.6)
I/σ ₁	18.8 (4.6)
Completeness (%)	98.2 (97.8)
Redundancy	12.3
Refinement	
Resolution (Å)	3.2
No. Reflections	13588
R _{work} /R _{free} (%)	22.1/26.1
No. Atoms	4798
Protein	4792
Ligand/ion	6
Avg. B-factor (Å ²)	50.1
R.m.s. deviations	
Bond lengths (Å)	0.004
Bond angles (°)	0.789

Values in parenthesis correspond to the highest resolution shell (3.4–3.2 Å)

a) $R_{pim} = \sum_{hkl} \{1/(N-1)\}^{1/2} \sum_i |I_i(hkl) - I(hkl)| / \sum_{hkl} \sum_i I_i(hkl)$, where *i* indexes the *i*th measurement of reflection *hkl* and *N* indicates the total number of times a given reflection is measured.